Revista Internacional de Ciencia y Tecnología de la Información Geográfica
International Review of Geographical Information Science and Technology

Oliva Pavón, P. y Chuvieco, E. (2013): "Assessment of the discrimination ability of MERIS spectral data for burned area mapping using ROC curves", GeoFocus (Artículos), nº 13-2, p. 41-65. ISSN: 1578-5157

ASSESSMENT OF THE DISCRIMINATION ABILITY OF MERIS SPECTRAL DATA FOR BURNED AREA MAPPING USING ROC CURVES

OLIVA PAVÓN, P.[1*], CHUVIECO SALINERO, E.[2**]
*Department of Geographical Sciences, College of Behavioral and Social Sciences, University of Maryland
4321 Hartwick Rd. Suite 209, College Park, 20740 Maryland (USA)
**Environmental Remote Sensing Research Group, Department of Geography and Geology, University of Alcala
Colegios 2, Alcalá de Henares, Madrid, 28801, Spain
[1] patricia.oliva@uah.es, [2] emilio.chuvieco@uah.es

ABSTRACT

Traditionally, the selection of the most appropriate bands to classify the target cover was supported by statistical indices that measured the discrimination ability of the spectral bands based on the Gaussian distribution assumption. However, that assumption might not be fulfilled in every instance. In this study we applied a non-parametric test (receiver operating characteristic, ROC) to measure the discrimination ability of MERIS sensor spectral bands and derived spectral indices to classify burned areas. The discrimination potential of each band was computed from the post-fire image, and from the temporal difference of the images. In both cases, the sources of confusion between burned areas and other covers were identified. The bands with higher discrimination ability were the NIR bands and the best indices were η, GEMI, BAI, α B8, α B10, DGEMI and DBAI.

Keywords: separability, non-parametric analysis, forest fires, satellite images.

ANALISIS DE LA CAPACIDAD DE DISCRIMINACIÓN DE LOS DATOS ESPECTRALES DEL SENSOR MERIS PARA LA CARTOGRAFÍA DE ÁREA QUEMADA UTILIZANDO CURVAS ROC

RESUMEN

Tradicionalmente, la selección de las bandas más apropiadas para la clasificación de coberturas específicas se realizaba a partir de índices estadísticos que medían la capacidad de discriminación de las bandas espectrales. Estos índices estadísticos asumían la distribución Gaussiana de los datos. Sin embargo, dicha asunción puede no cumplirse en todos los casos. En este estudio hemos aplicado un test no paramétrico (receiver operating characteristic, ROC) para medir la capacidad de discriminación de las bandas espectrales del sensor MERIS y de los índices espectrales derivados de ellas para la clasificación de áreas quemadas. El potencial de discriminación de cada banda fue calculado a partir de los datos procedentes de la imagen post-incendio y de la diferencia temporal de las imágenes. En ambos casos, las fuentes de confusión

Recibido: 8/02/2013
Aceptada versión definitiva: 26/06/2013

Oliva Pavón, P. y Chuvieco, E. (2013): "Assessment of the discrimination ability of MERIS spectral data for burned area mapping using ROC curves", GeoFocus (Artículos), nº 13-2, p. 41-65. ISSN: 1578-5157

entre las áreas quemadas y otras coberturas fueron identificadas. Las bandas con mayor poder de discriminación fueron las bandas del IRC y los mejores índices fueron η, GEMI, BAI, α B8, α B10, DGEMI and DBAI.

Palabras clave: separabilidad, análisis no paramétrico, incendios forestales, imágenes de satélite.

1. Introduction

Wildland fires are a very relevant factor of environmental change, causing loss of vegetation cover, alterations of vegetation succession patterns, changes in soil structure, and enhanced risk of water pollution (Pyne *et al.*, 1996; Viedma *et al.*, 2006). Moreover, biomass burning is an important source of greenhouse gas (GHG) emissions and a key input in climate models (van der Werf *et al.*, 2010). Accurate estimations of burned areas are essential to obtain a measurement of the surface area affected by fires and evaluate their effects on ecosystems and the chemical composition of the atmosphere.

Over the last decade numerous studies have made important advancements in the search for the best method to map burned areas. Those authors have applied and developed several techniques to detect fire-affected areas using different satellite sensors (Silva *et al.*, 2004; Roy *et al.*, 2005; Chuvieco *et al.*, 2008c; Tansey *et al.*, 2008; Giglio *et al.*, 2009).

More recently, several authors have used Medium Resolution Imaging Spectrometer (MERIS) data to map burned areas. MERIS provides better spatial resolution than MODIS (300 m), and narrower bands located between the blue and near infrared (490 – 900 nm). Oliva *et al.* (2011) studied the performance of several spectral indices derived from MERIS Full Resolution Level 2 data to map burned areas in the North-western part of the Iberian Peninsula during the 2006 fire season. They applied the spectral angle images (SAIs) technique to map burned areas following the method introduced by Oliva and Martin (2007). The SAIs measured the spectral angle between the spectral response of a pixel and the reference spectrum defining the spectral response of the burned area (Debba *et al.*, 2005). In this study they explored two reference spectra obtained from the image and from field spectral measurements. The highest accuracy was given by the SAI which used the reference spectrum obtained from the post-fire image. It showed omission and commission errors of 40% and 20%, respectively.

González-Alonso *et al*. (2009) used MERIS FR Level 1b data for burned area discrimination on a regional scale applying a hybrid method that combined active fire detection from a MODIS (Moderate Resolution Imaging Spectrometer) sensor product (MOD14) (Giglio *et al.*, 2003) and MERIS reflectances. This study was applied to the Province of Heilongiang in the North of China, in the framework of the ESA DRAGON-2 project. Basically, the algorithm consisted of finding the reflectance value in the NIR band of the post-fire image that maximized the agreement between the burned areas perimeters and the presence of active fires detected by MODIS. The resulting burned area maps were compared with the MODIS burned area product (MOD45) (Roy *et al.*, 2005) showing slight differences.

Oliva Pavón, P. y Chuvieco, E. (2013): "Assessment of the discrimination ability of MERIS spectral data for burned area mapping using ROC curves", GeoFocus (Artículos), nº 13-2, p. 41-65. ISSN: 1578-5157

On the other hand, MERIS images have also been used to estimate burn severity on a local scale showing high overall accuracy and good correlation with higher resolution data (Roldán-Zamarrón *et al.*, 2006; Gonzalez-Alonso *et al.*, 2007; De Santis and Chuvieco, 2008). These studies proved the potential of MERIS Full Resolution Level 1b data to detect differences in the level of damage produced by fire.

Even though MERIS does not acquire information in the SWIR region of the spectrum, which has proven to be very relevant for mapping burned areas (Eva and Lambin, 1998a; Pereira, 1999; Koutsias and Karteris, 2000; Roy and Landmann, 2005; Smith *et al.*, 2007), this sensor offers interesting possibilities for this task as it provides narrow bands and multiple observation channels on the red and near infrared. Specifically, MERIS is the only multi-spectral sensor which includes bands in the region known as red edge (690-770 nm). In this spectral region it is possible to observe the sharp increase of reflectance values between the red and the NIR regions which refers to healthy vegetation. Consequently, this region has been used to estimate chlorophyll content and to define different senescence phases in plants (Zarco-Tejada and Miller, 1999; Zarco-Tejada *et al.*, 2004). Therefore, MERIS data provide the opportunity to retrieve further information about the spectral characteristics of burned areas.

Traditionally, discrimination ability (DA) measures, also known as separability, have been used for selecting bands or spectral indices that better discriminate between different land cover classes. Most commonly, those metrics assume a Gaussian distribution of the probability functions of the land cover classes. The normalized distance (Kaufman and Remer 1994), the transformed divergence (Kumar and Silva, 1977), the Battacharrya distance (Kailath, 1967) and the Jeffries-Matusita distance (Richards, 1984) are the statistical measures more frequently applied (see table 2). In the case of burned area discrimination, the normalized distance (M) is the most utilized technique (i.e. (Pereira, 1999; Chuvieco *et al.*, 2002; Garcia and Chuvieco, 2004; Holden *et al.*, 2005; Smith *et al.*, 2007; Oliva *et al.*, 2011; Veraverbeke *et al.*, 2011) because it is simple to compute and interpret. However, this measure is very sensitive to the Gaussian assumption, and it would provide erroneous results when classes are skewed.

For this reason, we will be testing in this paper a new metric to measure the discrimination ability of MERIS spectral bands for burned area mapping. This non-parametric approach is called the receiver operating characteristic (ROC). This technique has been widely used in signal detection theory to evaluate classifiers, in medical diagnosis testing to analyse the behaviour of diagnostic systems, and recently in machine learning assessment (Swets *et al.*, 2000). ROC curves are insensitive to changes in class distributions and are not affected by skewed classes (Fawcett, 2006), which facilitate the comparison between classes with different probability distributions.

This paper computes ROC curves for MERIS original bands and derived indices to assess their discrimination ability and evaluate the sources of confusion that may affect the design of a burned area mapping algorithm.

2. Materials and methods

Oliva Pavón, P. y Chuvieco, E. (2013): "Assessment of the discrimination ability of MERIS spectral data for burned area mapping using ROC curves", GeoFocus (Artículos), nº 13-2, p. 41-65. ISSN: 1578-5157

2.1. Study area and dataset description

Two study sites commonly affected by severe fire seasons were selected for this article, both located in the Mediterranean Basin (figure 1). The first one covers Portugal and the Western region of Spain. The period selected corresponds to the fire season of 2005, which was one of the most severe in the last decade, affecting to more than 338000 ha of forested areas were burned which affected mostly shrublands, maritime pine (Pinus pinaster) and eucalyptus (Eucaliptus globulus).

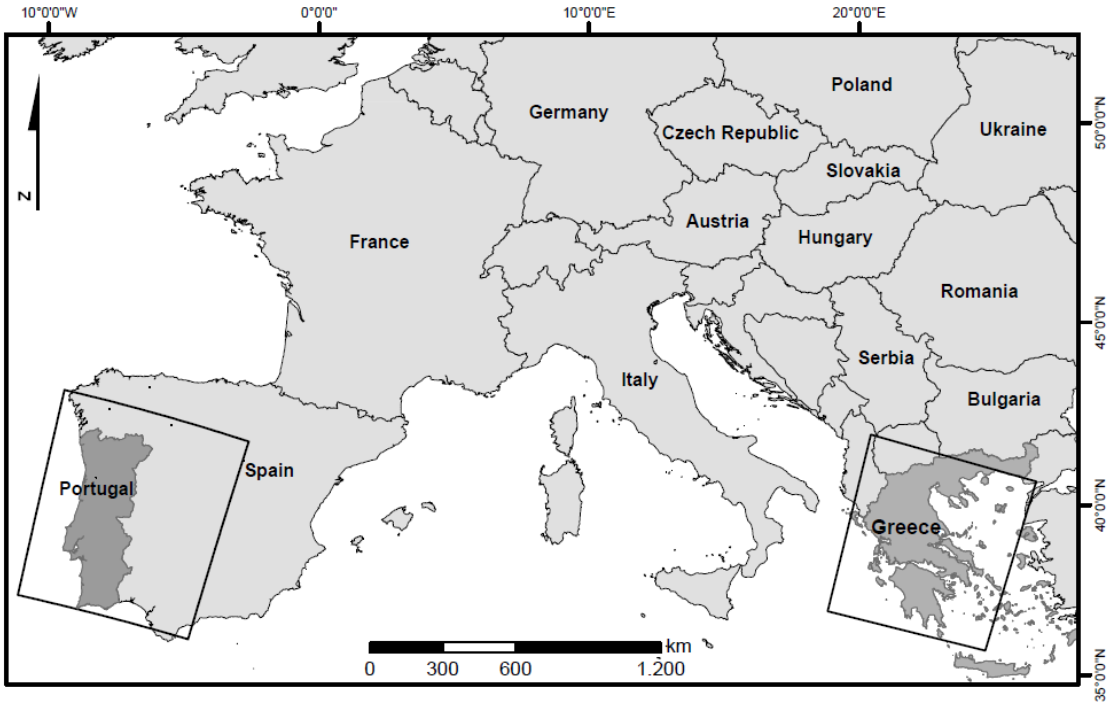

Figure 1. Study areas.

The second site covers most of the Greek Peninsula and the period selected was the fire season of 2007. Several massive forest fires occurred during the last weeks of August as a result of an intense heat wave. Most of the burned area was the result of 7 large fires, which burned 170000 ha, affecting approximately 60% of the forested areas of the southern region of Greece.

The data used in this study were acquired by the MERIS sensor, one of the ten instruments on board the ENVISAT (Environmental Satellite) of the European Space Agency. MERIS is an imaging spectrometer that measures the solar radiation reflected by the Earth at a ground spatial resolution of 300 meters in 15 spectral bands between 390 nm and 900 nm (Bézy *et al*., 2000) (table 1).

Oliva Pavón, P. y Chuvieco, E. (2013): "Assessment of the discrimination ability of MERIS spectral data for burned area mapping using ROC curves", GeoFocus (Artículos), nº 13-2, p. 41-65. ISSN: 1578-5157

Table 1. MERIS bands wavelength and spectral region

Spectral region	Blue			Green		Red			NIR						
MERIS band	B1	B2	B3	B4	B5	B6	B7	B8	B9	B10	B11	B12	B13	B14	B15
λ (nm)	412.5	442.5	490	510	560	620	665	681	708.75	753.75	760.62	778.75	865	885	900

We requested the most suitable Full Resolution (FR) MERIS images through a Cat-1 proposal granted by the European Space Agency. The FR Level 1b selected product includes top of the atmosphere reflectance of the 15 MERIS spectral bands at 300 meters. The images were atmospherically corrected applying the SCAPE-M routine (Guanter *et al.*, 2008). Two images of each study area, before and after the fire season, were selected so that the multi-temporal and post-fire burned area signal could be analysed (table 2).

Table 2. MERIS FR 1b data used for the burned area mapping algorithm calibration

Study area	**Fire season**	**Acquisition date (MM/DD/YYYY)**	**Product**	**Projection**
Portugal	2005	07/05/2005	MERIS FR 1b	UTM 29 T WGS 84
Portugal	2005	09/19/2005	MERIS FR 1b	UTM 29 T WGS 84
Grecia	2007	07/07/2007	MERIS FR 1b	UTM 34 T WGS 84
Grecia	2007	09/18/2007	MERIS FR 1b	UTM 34 T WGS 84

2.2. Sample selection

The CORINE Land Cover 2000 (30 m of spatial resolution) was used as a reference map to discriminate between different land cover types. The original classification of the CLC-2000 (44 categories) was simplified to 12 categories, from which 7 were selected to perform our analysis: forest, shrubland, grassland, cropland mosaic, rainfed cropland, irrigated cropland, and non-combustible areas. The categories urban, mineral, burnt, wetlands and water bodies were removed because afterwards a mask was applied to eliminate these areas.

A random sample of 200 points was extracted from each of the seven categories. The points were forced to be 600 m apart in order to avoid spatial correlation. On the other hand, an interior buffer of 100 m was established in each category to assure the selection of the targeted cover. This sample was obtained in both study areas, so a total of 400 points per category were finally processed.

Regarding the burned area sample, 200 points were extracted in both study sites using the burned area reference perimeters. The reference perimeters were obtained from the Rapid Damage Assessment service of the European Forest Fire Information System (EFFIS). These perimeters are digitized from MODIS images at 250 m spatial resolution. The fire perimeters were selected for each study area within the time frame established by the satellite images used in this study (table 2). An interior buffer of 100 meters was also considered in these perimeters, but the restriction of the

Oliva Pavón, P. y Chuvieco, E. (2013): "Assessment of the discrimination ability of MERIS spectral data for burned area mapping using ROC curves", GeoFocus (Artículos), nº 13-2, p. 41-65. ISSN: 1578-5157

distance between points was reduced to 300 meters in this case in order to obtain the number of points required to perform the statistical analysis.

2.3. The ROC curves

The ROC curve determines the accuracy of a binomial classification by measuring the overlap between two categories. There are four possible outcomes when assessing the accuracy of a classification model, which are represented in a confusion matrix (table 3). Following the terminology presented by Fawcett (2006), the reference data (true class) will be referred to as positive (P) or negative (N), and the classified or predicted classes will be named "y" or "n". If the instance is positive and it is classified as positive, it will be counted as a true positive (TP); if it is classified as negative, it will be counted as false positive (FP). On the other hand, if the instance is negative and it is classified as negative, it will be counted as a true negative (TN); if it is classified as positive, it will be counted as false negative (FN) (table 3). In this study, we obtained the reference data from the sample selection explained in section 2.2 where we considered as positive the burned area sample and as negative the rest of the covers.

Table 3. Confusion matrix used to compute the ROC curves. TPR stands for true positive ratio and FPR stands for false positive ratio

		Reference	
		Positive	**Negative**
Classified	**y**	True Positive (TP)	False Positive (FP)
	n	False Negative (FN)	True Negative (TN)
	Total	P=TP + FN	N=FP + TN

$$FPR = \frac{FP}{N} \qquad specificity = 1 - FPR$$

$$TPR = \frac{TP}{P} \qquad precision = \frac{TP}{TP + FP}$$

The ROC curves are then constructed by establishing consecutive instances defined by a threshold in the chosen variable. The TPR (True positive ratio) and the FPR (False positive ratio) of these instances are computed and represented to build the ROC curve (figure 2). That is to say that a certain threshold in the variable produce a number of points properly classified (counting both classes of the binomial classification) and a number of points misclassified. These numbers are used to compute the TPR (or hit rate) and the FPR (or error rate). Therefore, ROC curves represent the rate of correctly identified positives related to the misclassified negative instances, also called false alarms (Fawcett, 2006).

The diagonal, from the coordinate (0,0) to (1,1), represents those instances where the TPR is the same as the FPR, meaning that there is no separation between the two classes. The more asymptotic the curve the better the discrimination between the classes. Consequently, there is complete separation between the two classes when the curve passes through the coordinates (0,1) and (1,0).

Oliva Pavón, P. y Chuvieco, E. (2013): "Assessment of the discrimination ability of MERIS spectral data for burned area mapping using ROC curves", GeoFocus (Artículos), nº 13-2, p. 41-65. ISSN: 1578-5157

The area under the ROC curve (AUC) is the statistic that measures the discrimination ability between two probability distributions. As the diagonal marks the overlap between probability distributions, which has an area of 0.5, the separation of both probability distributions will be higher as the ROC curve is located further away from the diagonal. In terms of discrimination ability AUC values lower than 0.5 also indicate the separation between the probability distributions but in the opposite direction. The closer to one and zero, the higher the discrimination between classes. Consequently, we defined the discrimination index (DI) as the absolute value of the difference between the AUC value of the index and the AUC value of the diagonal, namely 0.5. Therefore, the DI varies between 0 and 0.5. Then, the closer to 0.5 the higher the discrimination ability.

$$DI = |AUC - 0.5|$$

Following the example displayed on figure 2, the DI of the high discrimination curve is 0.4, the medium discrimination DI value is 0.2 and the diagonal DI value is 0.

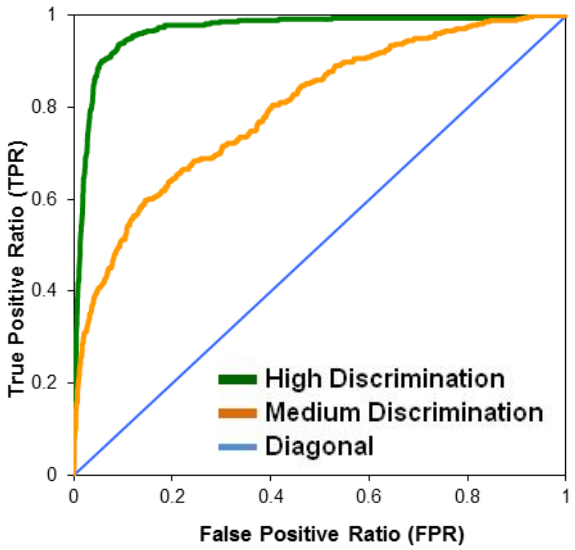

Figure 2. Graphic display of ROC curves. The area under the curve values of these curves are as follow, high discrimination curve AUC=0.9, the medium discrimination curve AUC=0.7 and diagonal AUC=0.5. The diagonal represents the situation where there is no separation between the two classes.

Besides the AUC value, the shape of the ROC curve can also provide useful information. Figure 3 illustrates a case where two classifiers, A and B, have the same AUC value but the shape of the ROC curve is complementary. Both classifiers perform the classification between two categories (1 and 2). We consider category 1 as the category of interest. Classifier A shows a higher slope than B at the bottom-left corner of the curve, thus A is able to classify category 1 with a higher hit rate, producing a lower error rate. On the other hand classifier B achieves higher values of TPR than A when the FPR is higher than 0.4. This means that classifier B performs a better

Oliva Pavón, P. y Chuvieco, E. (2013): "Assessment of the discrimination ability of MERIS spectral data for burned area mapping using ROC curves", GeoFocus (Artículos), nº 13-2, p. 41-65. ISSN: 1578-5157

classification of category 2 than the classifier A at error rates higher than 0.4. Considering the burned area as category 1, classifier A would correctly classify the 60% of the burned area producing a lower error than classifier B (<20% error or FPR<0.2). However, to correctly classify the 90% of the burned area classifier B would offer lower error rates than classifier A (60% and 90%, respectively). The two classifiers are valid, but the objectives of the study will justify the selection of one of them. In this case we look for a variable that provides a high discrimination of the burned area category, thus focusing attention on the bottom-left corner of the curves.

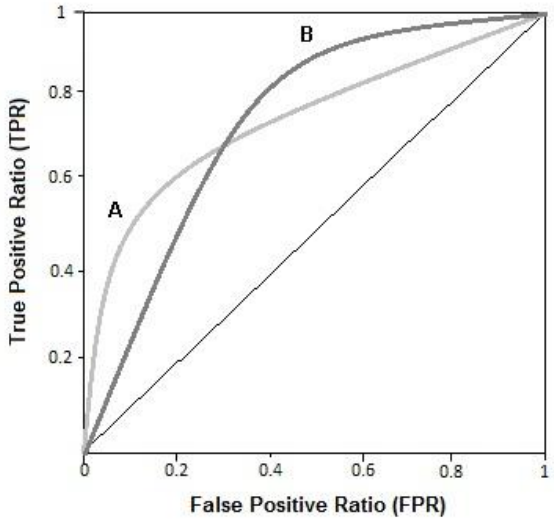

Figure 3. Analysis of the shape of ROC curves with equal AUC values. A and B curves represent two possible ROC curves from two classification methods. Both ROC curves, A and B, have the same value of area under the ROC curve which means that both classifications offer the same accuracy.

In order to detect the variables with higher precision we established a fixed FPR value of 0.05 (5% error) and observed the TPR values of the ROC curves computed for the different variables considered in this paper. The true positive rate, also referred to as the "hit rate", indicates the proportion of the sample correctly classified. Therefore, the variables that can correctly classify a higher rate at a low error rate will be defined as appropriate to identify burned areas. In other words, the variables will be able to correctly classify a higher proportion of burned pixels producing very low errors.

2.4. Spectral indices

After a fire there is a systematic drop in the reflectance in the NIR region. This spectral change produced after a fire is exploited by spectral indices. The spectral characteristics of the MERIS sensor make possible to explore the best red-NIR band combination to detect burned areas. In consequence this paper studied the discrimination ability of various spectral indices taking into account several red-NIR band combinations (table 4). These indices were selected from the analysis

Oliva Pavón, P. y Chuvieco, E. (2013): "Assessment of the discrimination ability of MERIS spectral data for burned area mapping using ROC curves", GeoFocus (Artículos), nº 13-2, p. 41-65. ISSN: 1578-5157

of papers related to burned area mapping (Eva and Lambin, 1998a; Chuvieco *et al*., 2002; Holden *et al*., 2005; Smith *et al*., 2007).

The Global Environmental Monitoring Index (GEMI) was used in burned area mapping for its non-linear variation, which provides greater sensitivity than other indices at low R-NIR reflectances (Pereira, 1999; Kucera and Yoshifumi, 2001; Chuvieco, 2002; Chuvieco *et al*., 2008a). Although GEMI was designed for AVHRR, some studies use its formula with different sensors (Maggi and Stroppiana, 2002; Stroppiana *et al*., 2002; Oliva *et al*., 2011). We included in our analysis the η intermediate index as well, as it had shown good performance in previous burned area studies (Oliva *et al*., 2011).

Table 4. Vegetation spectral indices used in this study

Index	Formula
Global Environmental Monitoring Index (Pinty and Verstraete, 1992)	$GEMI = \eta(1-0.25\eta) - \left[(\rho_R - 0.125)/(1-\rho_R)\right]$ $\eta = \frac{2(\rho_{NIR}^2 - \rho_R^2) + 1.5\rho_{NIR} + 0.5\rho_R}{\rho_{NIR} + \rho_R + 0.5}$
	Where ρ_R and ρ_{NIR} are the reflectance in the red and NIR region
Burned Area Index (Martín ,1998)	$BAI_i = \frac{1}{(\rho c_R - \rho_R)^2 + (\rho c_{NIR} - \rho_{NIR})^2}$
	Where ρ_R and ρ_{NIR} are the reflectance in the red and NIR region, and pc_R and pc_{NIR} are convergence points in the red and NIR region, respectively. In the original formulation the *pc* value was 0.1 in the red and 0.06 in the NIR.

The BAI index was formulated by Martín (1998) as the inverse of the Euclidean distance between the reflectance values in the red and NIR bands, and the convergence points, which were empirically-determined to define the average spectral response of charcoal. This index was developed with AVHRR data, but it has been successfully applied in several sensors such as Landsat-TM, MODIS, SAC-C and MERIS (Chuvieco *et al*., 2002; Garcia and Chuvieco, 2004; Chuvieco *et al*., 2008b; Oliva *et al*., 2011). However, given the particular characteristics of MERIS bands, their location in the spectrum and their narrow band width, we considered appropriate to re-calculate the convergence points in order to improve the performance of the BAI index. The convergence points were estimated empirically using the 5th percentile value in the red region and the 95th percentile in the NIR region from a random sample of burn pixels. This criterion was defined according to the direction of change of the vegetation spectral response after being affected by fire.

2.5. Hyperspectral indices

Although the MERIS sensor is not properly a hyperspectral sensor, its 15 bands and narrow bandwidth place it close to hyperspectral data. We tested two hyperspectral techniques, the

Oliva Pavón, P. y Chuvieco, E. (2013): "Assessment of the discrimination ability of MERIS spectral data for burned area mapping using ROC curves", GeoFocus (Artículos), nº 13-2, p. 41-65. ISSN: 1578-5157

continuum removal and the inter-band angle, and evaluated the ability of these techniques to detect burned areas.

The continuum spectrum is defined as a convex "helmet" formed by the lines linking the points of maximum reflectance of a single spectrum (Clark and Roush, 1984). In this study the continuum removal was computed by dividing the original spectrum by the continuum spectrum. That way a normalized spectrum was obtained where the absorption bands were enhanced. This technique has been widely used in geological studies and vegetation mapping, as well as to estimate the concentration of some chemical components in the leaves (van der Meer, 2000; Curran *et al*., 2001; Huang *et al*., 2004; Mutanga *et al*., 2004). Some authors highlighted that the limitation of the spectral range avoids the interference from adjacent absorption bands (van der Meer, 2000; Mutanga *et al*., 2004). Therefore, we limited the continuum removal computation from band 5 (510 nm) to band 10 (753.75 nm). Changes in the absorption band located in the red spectral region were enhanced after the continuum removal process (figure 4).

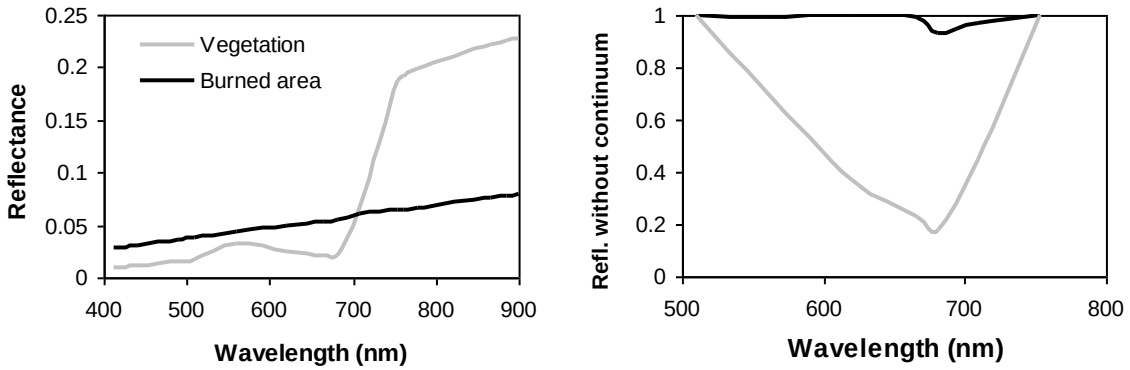

Figure 4. Example of the continuum removal technique which shows the temporal evolution of a vegetated pixel before and after a fire event.

To date the MERIS sensor is the only multi-spectral medium resolution sensor with narrow bands which are close enough to detect absorption bands and estimate its depth. The depth of the absorption band in the red is given by the reflectance value without continuum in band 8 (681.25 nm). We also computed the slope between bands 8 and 10 with the continuum removed.

The other technique applied was adapted from Khanna et al. (2007) who introduced the definition of two new spectral indices based on the cosine theorem. This theorem establishes how to compute the angle centred in one of the vertices of a triangle from the longitude of its sides. Accordingly, three consecutive bands are required to compute this index (figure 5). The angle computed corresponds to the central band of the three bands selected. The location of those bands in the spectrum is also a key factor since their wavelength establishes the kind of information that is included in a band. As our purpose was to detect burned areas, we focused on the regions where the changes between green vegetation and burned areas were more noticeable: the absorption band in the red centred at band 8 (681 nm), and the "shoulder" in the NIR where the slope of the green vegetation spectra changes abruptly, centred at band 10 (758.75 nm). The red bands selected to

Oliva Pavón, P. y Chuvieco, E. (2013): "Assessment of the discrimination ability of MERIS spectral data for burned area mapping using ROC curves", GeoFocus (Artículos), nº 13-2, p. 41-65. ISSN: 1578-5157

compute the angle were bands 6, 8 and 9 (620, 681, and 708.75 nm), and the NIR bands selection was formed by bands 9, 10 and 12 (708.75, 758.75, and 778.75 nm).

The formula to compute the band angle index is defined as follows:

$$\alpha = \cos^{-1}\left[\frac{a^2 + b^2 - c^2}{2ab}\right](radians)$$

Where a, b and c are computed as Euclidean distances between the vertices. a and b represent the length of the sides and c represents the length of the side opposite to the angle we want to compute. The Euclidean distance is defined as,

$$d = \sqrt{(\rho_1 - \rho_2)^2 + (\lambda_1 - \lambda_2)^2}$$

Where ρ1 and ρ2 are the reflectance values of bands 1 and 2 from 0 to 1, and λ1 and λ2 the corresponding wavelength in micrometres.

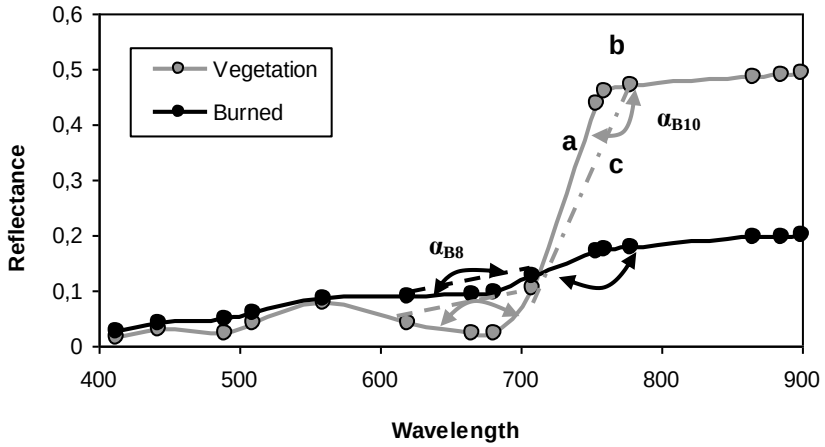

Figure 5. Angle indices in the red and in the red edge of two spectra: green vegetation (grey line) and burned area (black line). Dashed lines mark the limits of the triangle formed by the three bands considered. The bullets mark the location of the MERIS bands.

3. Results

3.1. Band discrimination ability

Figure 6 displays the values of the discrimination index (DI) using each band as a variable to discriminate between burned areas and each land cover. In general, the Portugal-2005 sample showed higher values of DI than the Greece-2007 sample in every land cover. In addition, the NIR

Oliva Pavón, P. y Chuvieco, E. (2013): "Assessment of the discrimination ability of MERIS spectral data for burned area mapping using ROC curves", GeoFocus (Artículos), nº 13-2, p. 41-65. ISSN: 1578-5157

bands showed the highest DI in every category in both samples, meaning that their discrimination ability is very high.

The categories that showed larger differences between the two study sites were cropland mosaic, forest and shrubland. These differences range from 0.1 to 0.4 and are located in the visible region of the spectrum. In the case of cropland mosaic, the DI of Greece is particularly low in the blue bands since it is not higher than 0.3. In the red bands the DI value of the Greece sample it is also low since it has a value of 0.3. However, the DI values in the cropland mosaic of Portugal are always close to the maximum value of 0.5.

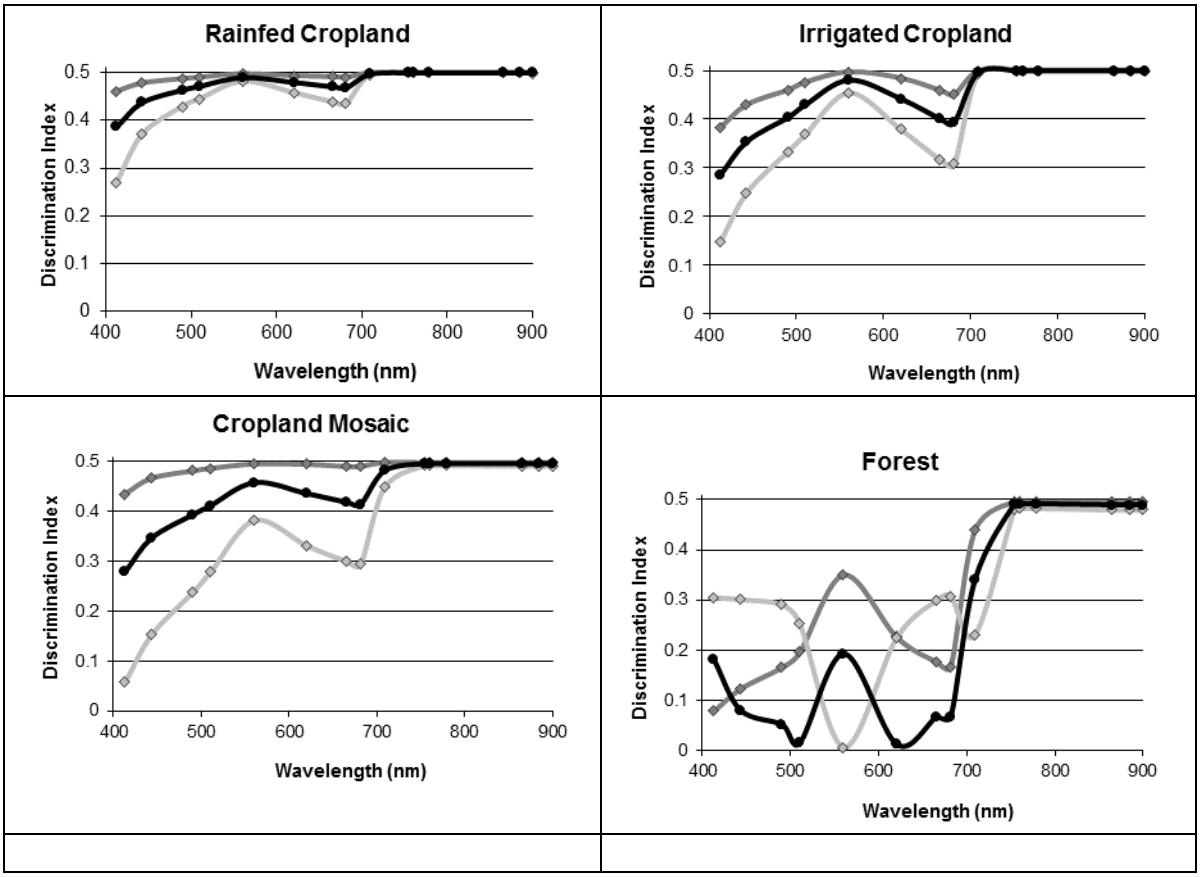

Oliva Pavón, P. y Chuvieco, E. (2013): "Assessment of the discrimination ability of MERIS spectral data for burned area mapping using ROC curves", GeoFocus (Artículos), nº 13-2, p. 41-65. ISSN: 1578-5157

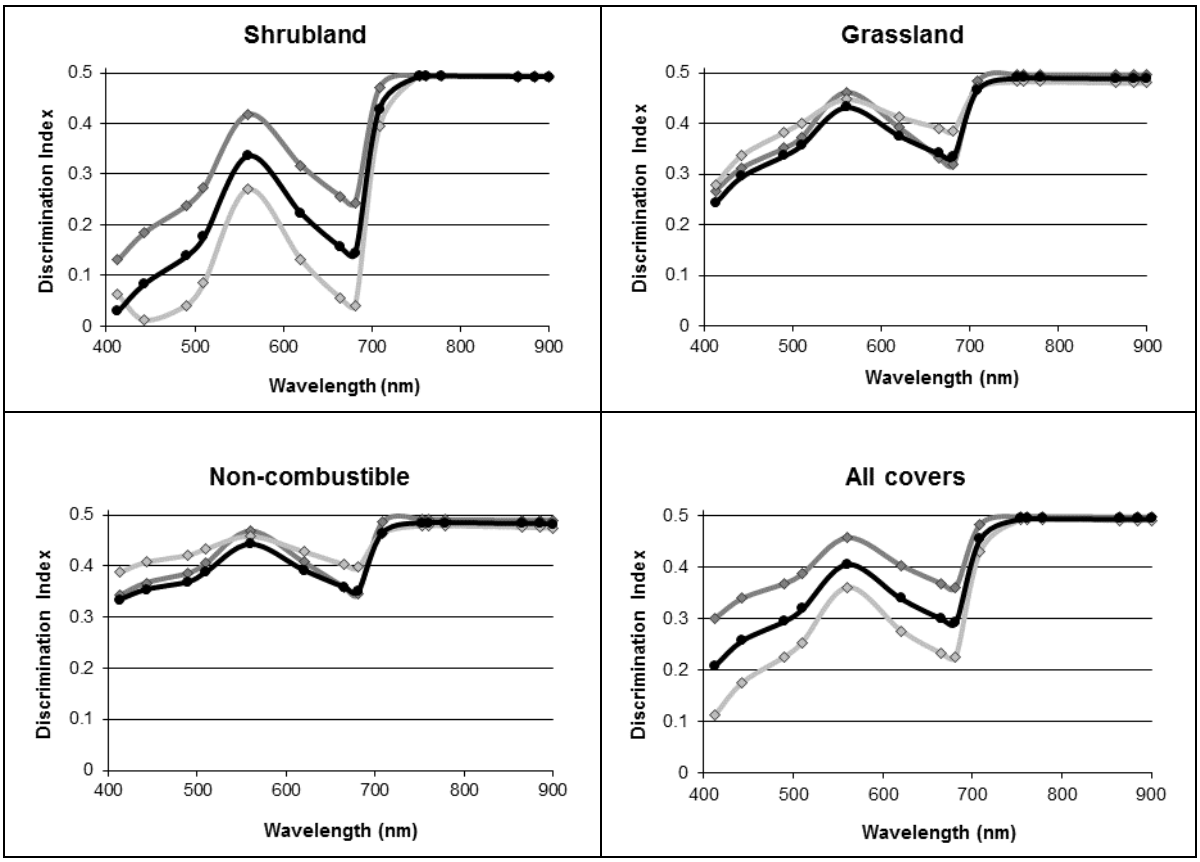

Figure 6. Discrimination Index computed from the AUC of the ROC curves between burned areas and land cover categories in the post-fire sampled data from Portugal-2005 (dark grey line), Greece-2007 (light grey line) and the joint dataset (black line). The DI represents the ability to discriminate burned areas, where 0 means no discrimination and 0.5 means maximum discrimination.

In the shrubland category the difference between Portugal and Greece is consistent throughout the bands in the visible region. Therefore, the Greece DI values are 0.2 lower than the Portugal DI values.

The DI values in the forest category showed a particular behaviour. In the Portugal-2005 sample the DI values showed low DI in the visible region with the exception of band 5 (560 nm) which showed a DI value of 0.35. In comparison the DI values of the Greece-2007 sample are mostly around 0.3 with the exception of band 5 that showed the lowest DI.

On the other hand, in the rest of the land cover categories the results showed very high AUC values in the NIR bands and lower values in the visible region of the spectrum with a relative peak in the green bands. Although the red bands showed lower DI values than the NIR bands, they displayed generally high DI in most of the covers, except in forest and shrubland.

Oliva Pavón, P. y Chuvieco, E. (2013): "Assessment of the discrimination ability of MERIS spectral data for burned area mapping using ROC curves", GeoFocus (Artículos), nº 13-2, p. 41-65. ISSN: 1578-5157

In the temporal difference analysis (TDA) we observed very high values of DI from band 10 (758.75 nm) onwards. Regarding the blue bands, the DI values varied from 0.1 to 0.3 in every category. The green bands showed the lowest values of DI, offering values close to zero. Whereas, the higher DI values among the visible bands were given by the red bands which offered values higher than 0.35. In this analysis the NIR bands showed also DI values higher than 0.4, with the exception of the irrigated cropland category.

The most significant difference between study areas appeared in the red bands. While the Portugal DI values in the red bands were generally higher than 0.3, in the Greece sample the DI values were lower than 0.1.

The land covers which offered higher variability between study areas were rainfed cropland, forest, shrubland, grassland and non-combustible. In this case the Portugal sample showed higher DI than the Greece sample in the blue and red bands. Whereas, the Greece sample offered higher DI values in bands 5 and 9.

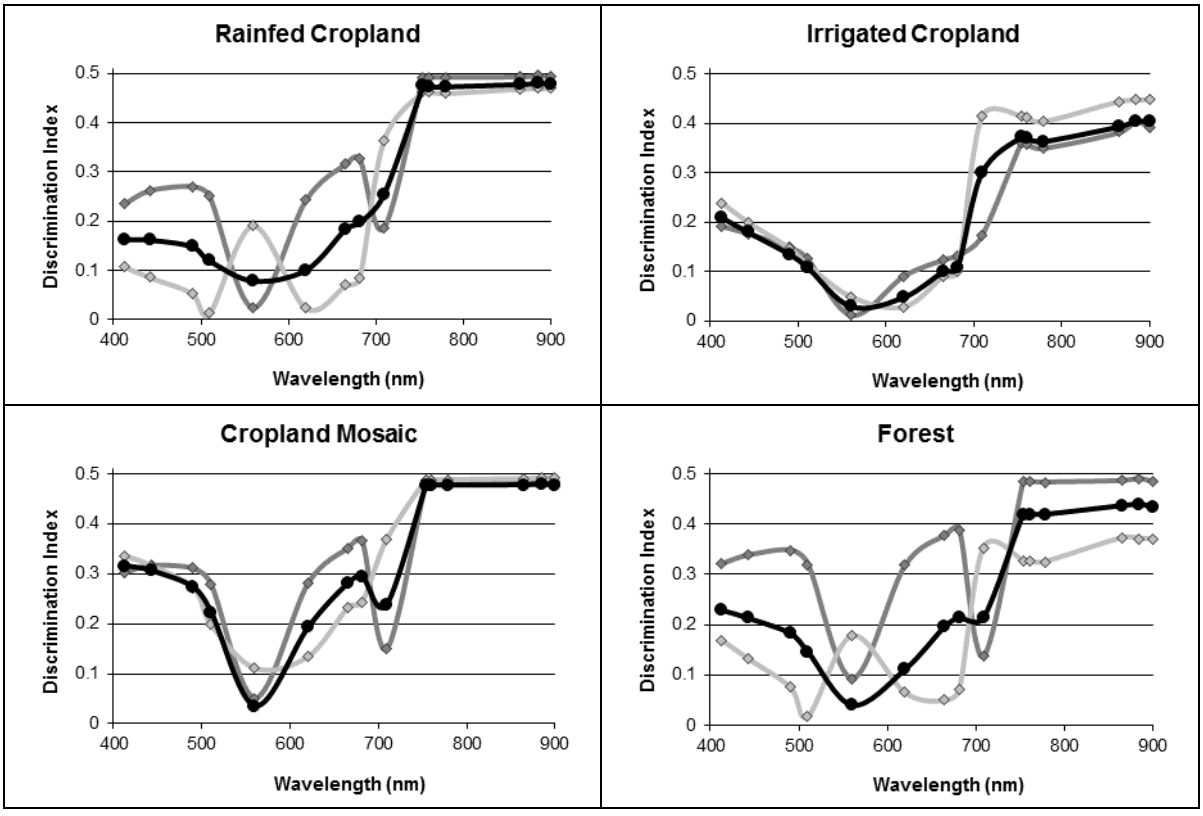

Oliva Pavón, P. y Chuvieco, E. (2013): "Assessment of the discrimination ability of MERIS spectral data for burned area mapping using ROC curves", GeoFocus (Artículos), nº 13-2, p. 41-65. ISSN: 1578-5157

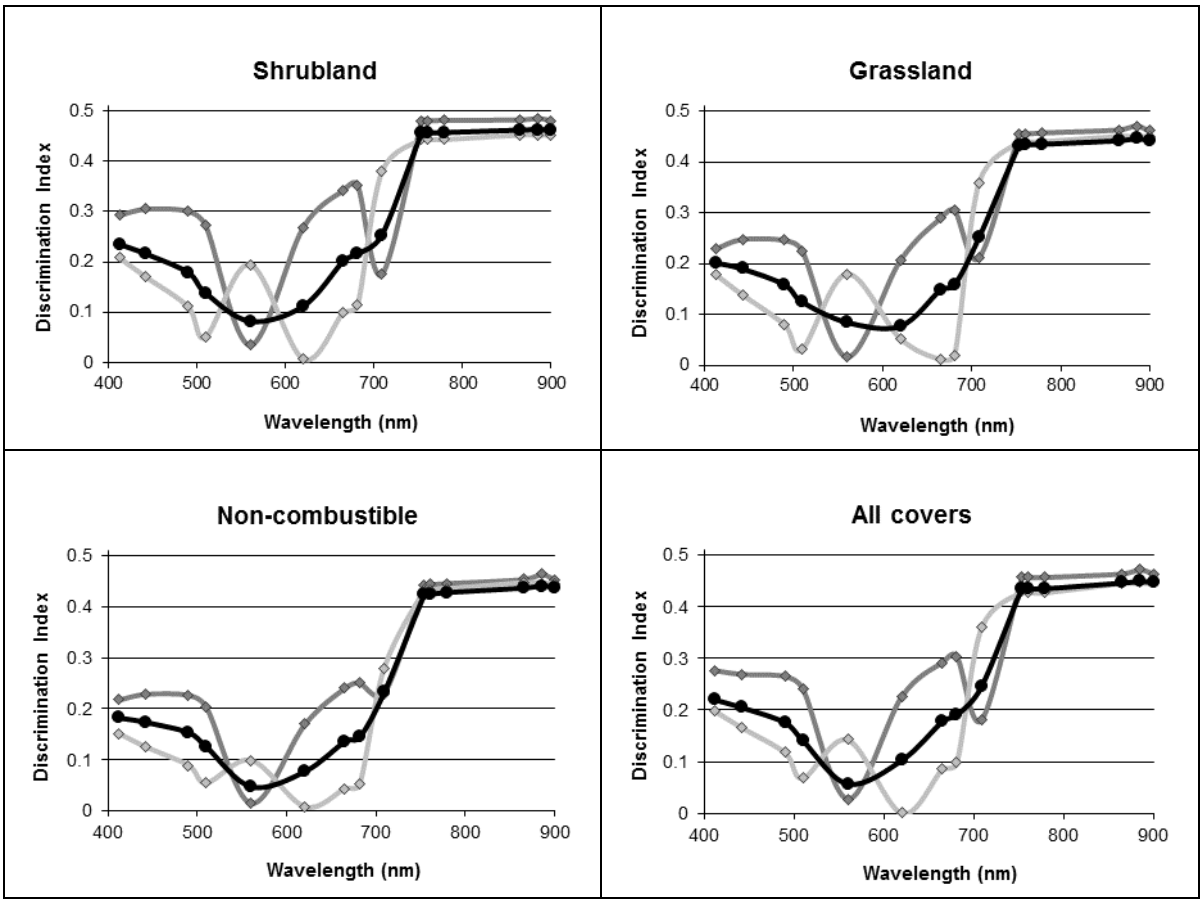

Figure 7. Discrimination Index computed from the AUC of the ROC curves between burned areas and land cover categories in the temporal difference sampled data from Portugal-2005 (dark grey line), Greece-2007 (light grey line) and the joint dataset (black line). The DI represents the ability to discriminate burned areas, where 0 means no discrimination and 0.5 means maximum discrimination.

As a result of the discrimination ability analysis, we selected bands with the highest DI to build spectral vegetation indices. In the red region, the band 8 (681 nm) was selected because it showed DI values higher than 0.3 in most of the categories in the TDA and in the post-fire analysis. On the other hand, the NIR band selected was the band 14 due to the stability of its discrimination ability and the higher DI values showed in the TDA.

3.2. Discrimination analysis of the spectral indices

We computed the indices: η, GEMI and BAI from MERIS bands 8 (red) and 14 (NIR). In addition to these spectral indices, we computed the continuum removal from band 5 to band 10. We then selected the bands 7, 8 and 9 with their continuum removed (hereafter CR B7, CR B8 and CR

Oliva Pavón, P. y Chuvieco, E. (2013): "Assessment of the discrimination ability of MERIS spectral data for burned area mapping using ROC curves", GeoFocus (Artículos), nº 13-2, p. 41-65. ISSN: 1578-5157

B9), as well as the first derivative between bands 8 and 10 where the red edge slope is located. The band angle indices centred in band 8 and band 10 (hereafter α B8 and α B10) were also calculated.

ROC curves were computed in the post-fire and temporal difference analysis for every index and land cover. The values of DI obtained from the ROC curves are displayed in figure 8 showing the discrimination ability of the different variables. To discriminate temporal difference from the post-fire variables we added the letter "D" before the name of each index.

Comparing graphs A and B in figure 8 it may be observed that most spectral indices had higher values of DI than the hyperspectral indices in every land cover. On the other hand, there were not significant differences among spectral indices in the post-fire analysis (figure 8A). They showed DI values higher than 0.475 in every land cover which indicated very high discrimination ability.

In addition, the hyperspectral indices showed high variability of DI values. The DI values of the continuum removal indices were generally lower than the values of the band angle indices (figure 8B). In general, the hyperspectral indices showed low ability to discriminate rainfed croplands, with the exception of CR B7 and α10 which offered high DI values.

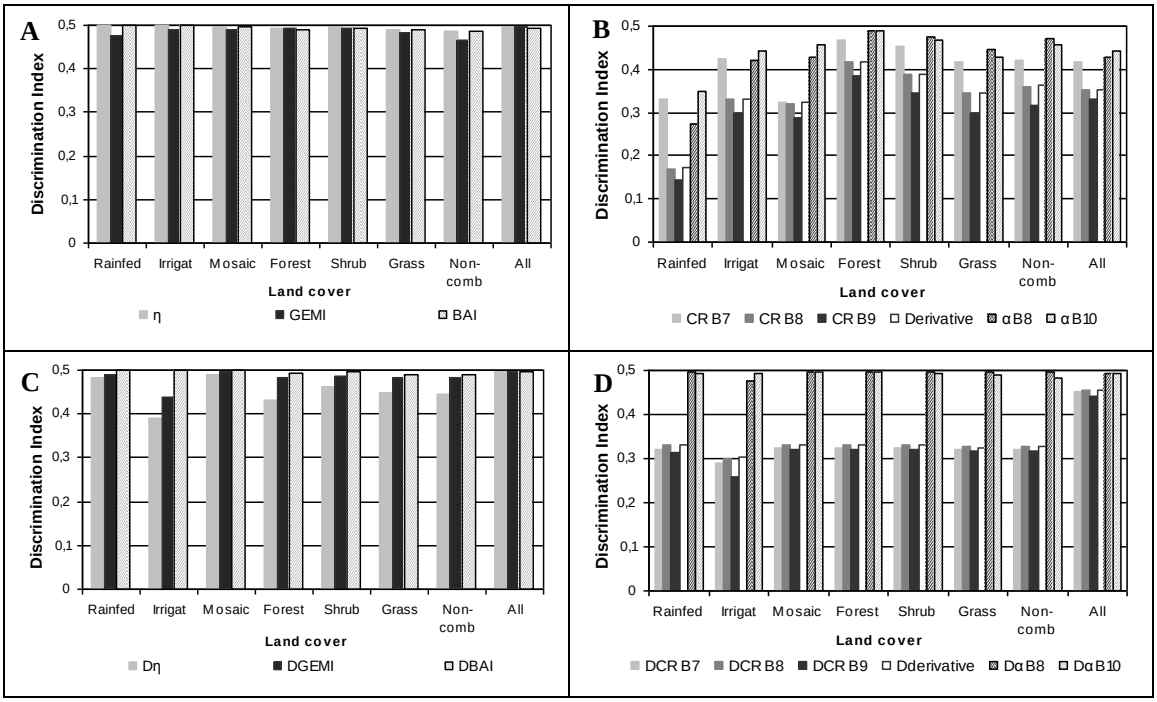

Figure 8. Discrimination Index (DI) of the ROC functions computed for every index by land cover. The DI represents the ability of the indices to discriminate burned areas, where 0 means no discrimination and 0.5 means maximum discrimination. Graphs A and B represent the post-fire analysis and graphs C and D refer to the temporal difference analysis.

Oliva Pavón, P. y Chuvieco, E. (2013): "Assessment of the discrimination ability of MERIS spectral data for burned area mapping using ROC curves", GeoFocus (Artículos), nº 13-2, p. 41-65. ISSN: 1578-5157

CR B7 offered a high overall discrimination ability even though the DI values of rainfed cropland and cropland mosaic were lower than 0.4. In the case of the band angle the differences between the two indices were not as high and their performance varied depending on the land cover. Both band angle indices showed DI values higher than 0.4 in every land cover with the exception of rainfed cropland, showing the highest overall discrimination ability within the hyperspectral indices.

The spectral indices continued showing high discrimination ability in the temporal analysis (figure 8C). The indices Dη and DGEMI obtained lower DI values in irrigated cropland compared to the rest of land covers. However, the DI was around 0.4 and the overall discrimination ability of the indices was not affected by this result.

On the other hand, the CR indices showed the lowest values of DI, around 0.3 in every land cover, which indicated a general decrease of the discrimination ability after performing the multi-temporal comparison of the images. On the other hand, the band angle indices showed very high DI values that matched the values of the best spectral index, in this case the BAI index. Therefore, the temporal difference of the image produced a notable increase in the DI of the band angle indices.

As explained in the previous section, the variables which would be selected as inputs for our burned area mapping algorithm must classify correctly a high percentage of burned area at a very low error rate. In order to check if they comply with this requirement, we retrieved the TPR corresponding to a fixed FPR of 0.05 from the ROC curves, which were previously computed from the whole dataset. This value (TPR) indicated the percentage of the sample that has been correctly classified (hit rate) when the error produced in the classification is 5%. Therefore, the higher the TPR the higher the discrimination ability. Figure 9 displays the TPR values (hit rate) of every index in the post-fire and temporal analysis.

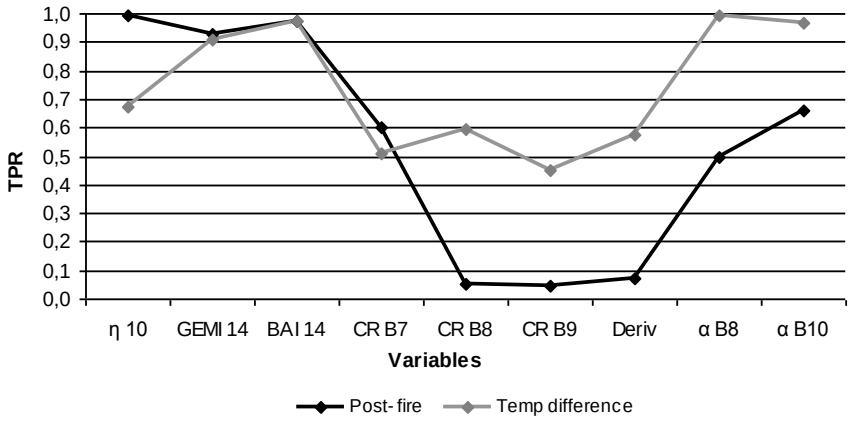

Figure 9. True positive fraction (TPR) or "hit rate" obtained at a fixed false positive ratio (FPR) of 0.05. The higher the value of TPR the higher the percentage of the sample correctly classified.

Oliva Pavón, P. y Chuvieco, E. (2013): "Assessment of the discrimination ability of MERIS spectral data for burned area mapping using ROC curves", GeoFocus (Artículos), nº 13-2, p. 41-65. ISSN: 1578-5157

In the post-fire analysis all the hyperspectral indices showed hit rate values lower than 0.7, while the spectral indices obtained hit rates higher than 0.9, which highlighted the differences between them. In other words, at a fix error rate of 5% the hyperspectral indices are able to correctly classify the 70% of the sample while the spectral indices achieved a 90%. Specifically, it was observed that the CR indices showed the lowest hit rate (< 0.1).

The TPR values obtained in the temporal analysis revealed that some variables offered a moderate hit rate (figure 9) despite showing very high values of DI (figure 8). This is the case of the spectral indices Dη 10, Dη 14 and DGEMI 10, which obtained TPR values lower than 0.85. On the other hand, CR indices showed medium TPR values which were in accordance with their DI values displayed in figure 8. Band angle indices obtained very high hit rate values, which demonstrated that they had a notable potential to discriminate burned areas.

4. Discussion

4.1. Band discrimination ability analysis

In the visible domain the DI values of the post-fire data were high in several covers, such as rainfed cropland, irrigated cropland, grassland and non-combustible areas. As we were evaluating an image acquired at the end of the dry season the spectral signature of crops and grassland corresponded to senescent vegetation or soil. Consequently, the green and red bands showed higher reflectance values in these covers than in burned areas. This effect was reflected in the post-fire image analysis in terms of high DI values in the green and red bands. The high discrimination ability found in these bands concurred with the results of previous studies which compared burned areas and senescent vegetation (Trigg and Flasse, 2001). On the other hand, the blue bands generally showed the lowest DI values. Specially, in the case of forest and shrubland covers the DI values of the blue bands were very low which concurred with the analysis of previous studies (Pereira, 1999; Garcia and Chuvieco, 2004; Smith *et al*., 2007; Oliva *et al*., 2011; Veraverbeke *et al*., 2011).

In the temporal difference analysis the DI values of the visible bands were low in most of the covers, meaning that they were not suitable to discriminate between these covers and burned areas. However, in the Portugal sample the red bands showed DI values higher than 0.3 in five of the seven covers analysed. Therefore these bands showed a moderate potential to discriminate burned areas.

Comparing the DI values of the visible bands in both study areas, we can observe notable differences between them in some covers. These differences revealed that despite being part of the same ecosystem there were substantial variations in the spectral response of vegetated land covers and burned areas in both study sites. These variations are influenced by several factors like vegetation type and characteristics, weather conditions, soil brightness and fire severity.

Oliva Pavón, P. y Chuvieco, E. (2013): "Assessment of the discrimination ability of MERIS spectral data for burned area mapping using ROC curves", GeoFocus (Artículos), nº 13-2, p. 41-65. ISSN: 1578-5157

The implicit variability included in these DI values pointed out one of the many difficulties involved in designing a global algorithm, because the same cover (i.e. forest) may have a very different spectral response in separate sites even though being part of the same ecosystem (Pereira, 1999; Silva *et al*., 2004). In consequence, it would not be advisable to use visible bands as a discrimination variable in global burned area mapping algorithms.

On the other hand, the NIR bands had stable and high DA values in both the post-fire and temporal analysis, demonstrating that they were the most suitable bands to detect burned areas, as shown in previous studies (Pereira, 1999; Koutsias and Karteris, 2000; Garcia and Chuvieco, 2004; Holden *et al*., 2005; Smith *et al*., 2007; Oliva *et a*l., 2011; Veraverbeke *et al*., 2011). In addition the differences between study areas did not affect the discrimination ability of the NIR bands. Because of that we stated that they were the most appropriate bands to be included in regional to global burned area mapping algorithms.

4.2. Index discrimination ability analysis

In the post-fire analysis the spectral indices (η, GEMI and BAI) showed higher values of DI than the hyperspectral indices in all the covers. In fact, the spectral indices had DI values higher than 0.95 in all the covers meaning that the discrimination ability of the indices was very high. In the case of the hyperspectral indices the higher values were displayed by the band angle indices (α B8 and α B10).

The high discrimination values of GEMI and BAI obtained in this study confirmed the results obtained in previous studies (Chuvieco *et al*., 2002; Garcia and Chuvieco, 2004; Oliva *et al*., 2011; Veraverbeke *et al*., 2011). However, there are also studies that showed low discrimination values for these indices (Smith *et al*., 2007; Veraverbeke *et al*., 2011). These studies used the normalized distance as a measure of the discrimination ability, which assumes the data adjust to a Gaussian probability distribution function. Consequently, the low values of normalized distance obtained in previous studies for the GEMI and BAI indices might be influenced by the non-Gaussian probability distribution of the data.

In the temporal difference analysis the spectral indices maintained their high DI values although there was a general decrease in the DI values of η and GEMI indices, especially in the irrigated cropland. The decrease in DI values of the irrigated cropland may be induced by the harvest of the crops in late summer. This event produced changes in the reflectance of these areas in the same direction that occurred after a fire event, showing higher reflectance values in the red bands and lower in the NIR bands. Although the decrease in the reflectance values was not as abrupt as that occurred when the vegetation was burned, this characteristic might introduce a source of confusion in burned area detection (Garcia and Chuvieco, 2004).

In this study BAI offered the highest DI values in all covers and the highest TPR in both post-fire and temporal analysis. These results indicated that BAI was the most suitable index to discriminate burned areas in both study sites. However, BAI has some limitations that were pointed

Oliva Pavón, P. y Chuvieco, E. (2013): "Assessment of the discrimination ability of MERIS spectral data for burned area mapping using ROC curves", GeoFocus (Artículos), nº 13-2, p. 41-65. ISSN: 1578-5157

out in previous studies (Garcia and Chuvieco, 2004; Oliva *et al.*, 2010), such as the systematic confusion with water bodies and cloud shadows.

The continuum removal indices showed in general low discrimination ability. Although, the CR B7 index offered DI values higher than 0.4 in five out of the seven categories in the post-fire analysis. The TPR value of the CR B7 index was 0.5, which meant that at a fixed error of 5% this index correctly classified only 50% of the sample. Therefore, we observed that the continuum removal indices were not adequate to classify burned areas. On the other hand, in the multi-temporal analysis the band angle indices, α B8 and α B10, had very high DI values, which matched the values obtained for the BAI index. These results proved the potential of these indices for burned area mapping.

Finally, from the TPR analysis we observed the proportion of the sample correctly classified by every index a fixed error rate of 5%. In the post-fire analysis, η, GEMI and BAI showed the best performances with TPR values higher than 0.9. In the multi-temporal analysis the indices with TPR values higher than 0.9 were GEMI, BAI, α B8 and α B10, which implies that these indices were able to correctly classify 90% of the sample producing an error rate of 5%. The TPR analysis offered a measure of the potential accuracy that may be obtained using a certain index as a classification variable. However, the results obtained from this analysis should be handled with care, since the TPR is computed from a sample of pixels.

Finally, from the TPR analysis we observed the proportion of the sample correctly classified by every index a fixed error rate of 5%. In the post-fire analysis, η, GEMI and BAI showed the best performances with TPR values higher than 0.9. In the multi-temporal analysis the indices with TPR values higher than 0.9 were GEMI, BAI, α B8 and α B10, which implies that these indices were able to correctly classify 90% of the sample producing an error rate of 5%. The TPR analysis offered a measure of the potential accuracy that may be obtained using a certain index as a classification variable. However, the results obtained from this analysis should be handled with care, since the TPR is computed from a sample of pixels.

The assessment of the different indices in post-fire and multi-temporal conditions allowed the selection of the best indices according to the objectives of the next analysis to be performed. The indices selected were η, GEMI, BAI, α B8, α B10, DGEMI and DBAI. These indices showed stable high discrimination ability in all the covers and a hit rate higher than 0.9.

Measuring the discrimination ability using ROC curves allowed (i) avoiding limitations related to the non-parametric probability distribution of the data, (ii) obtaining a discrimination values with a delimited range that enables comparison of index performance, and (iii) obtaining a measure of the potential classification accuracy. These properties make ROC curves an advisable technique to measure the discrimination ability between two categories.

In this study we have stated that even though MERIS sensor lacks SWIR bands there are suitable indices that can be used to classify burned areas corroborating the findings of Oliva et al. (2010). Currently, MERIS images are no longer available, as in April 2012 the ENVISAT satellite stopped communicating with ground stations. However, the ESA has planned a continuity mission

Oliva Pavón, P. y Chuvieco, E. (2013): "Assessment of the discrimination ability of MERIS spectral data for burned area mapping using ROC curves", GeoFocus (Artículos), nº 13-2, p. 41-65. ISSN: 1578-5157

called Sentinel-3 that includes an instrument called Ocean and Land Colour Instrument (OLCI) which is an enhance version of the MERIS sensor. This will open new possibilities for post-fire effects assessment on a global scale. Actually, as a part of the European Space Agency (ESA) Climate Change Initiative (CCI) the Fire Disturbance project is currently producing a global burned area mapping algorithm using MERIS, AATSR and SPOT-VGT imagery (www.esa-fire-cci.org). The results of this study were used by the Fire Disturbance project as a starting point focusing efforts on the bands and indices that showed the highest discrimination ability.

5. Conclusions

ENVISAT-MERIS (Medium Resolution Imaging Spectrometer) is not as well-known and used as other sensors frequently used in burned area mapping like MODIS, SPOT-VGT or AATSR. As displayed in table 1 MERIS sensor lacks SWIR bands. That is considered its main drawback, since those bands were proven to be very useful to map burned areas (López García and Caselles, 1991; Koutsias and Karteris, 1998; Trigg and Flasse, 2000; Holden *et al*., 2005; Smith *et al*., 2007). Nevertheless MERIS overcomes that drawback with 15 narrow spectral bands in the visible-NIR spectral region. The narrowness and the frequency of its bands make possible to apply hyper-spectral techniques, such as analysis of the absorption bands, and continuum removal, opening a range of new possibilities.

The discrimination ability analysis was performed by applying the ROC (Receiver Operating Characteristic) a non-parametric technique. It was selected since most of the indices showed a probability distribution that significantly differed from a Gaussian distribution. ROC curves allowed (i) computing the discrimination ability of non-parametric distributed data, (ii) obtaining a delimited range index that enables comparison of index performance, and (iii) obtaining a measure of the potential performance of the classification.

The results of this study demonstrated that in the context of burned area applications bands in the visible spectral region were not suitable to classify burned areas due to their low discrimination ability. In contrast, NIR bands offered stable and high discrimination ability, which made these bands adequate for temporal series analysis. Among the assessed indices, GEMI and BAI showed the higher discrimination ability in both post-fire and temporal analysis. In addition, band angle indices revealed a high potential for burned area mapping considering a multi-temporal analysis. Although these results should be handled with caution when applying these indices to other regions, our findings demonstrated the potential of MERIS bands to map burned areas.

Acknowledgements

The study has been funded by the Spanish Ministry of Education and Science by the scholarship granted to P. Oliva. The authors would like to thank the ESA for the MERIS images provided by a Cat-1 proposal.

Oliva Pavón, P. y Chuvieco, E. (2013): "Assessment of the discrimination ability of MERIS spectral data for burned area mapping using ROC curves", GeoFocus (Artículos), nº 13-2, p. 41-65. ISSN: 1578-5157

References

Bézy, J. L., S. Delwart, *et al*. (2000): "MERIS - A new generation of ocean-color sensor onboard Envisat", *ESA Bulletin*, 103, pp. 48-56.

Chuvieco, E. (2002): *Teledetección ambiental: La observación de la Tierra desde el espacio*. Barcelona, Ariel Ciencia.

Chuvieco, E., P. Englefield, *et al*. (2008a): "Generation of long time series of burn area maps of the boreal forest from NOAA-AVHRR composite data", *Remote Sensing of Environment*, 112, pp. 2381-2396.

Chuvieco, E., M. P. Martín, *et al*. (2002): "Assessment of different spectral indices in the red-near-infrared spectral domain for burned land discrimination", *International Journal of Remote Sensing*, 23, 23, pp. 5103-5110.

Chuvieco, E., S. Opazo, *et al*. (2008b): "Global burned-land estimation in Latin America using MODIS composite data", *Ecological Applications*, 18, 1, pp. 64-79.

Chuvieco, E., S. Opazo, *et al*. (2008c): "Global burned land estimation in Latin America using MODIS composite data", *Ecological Applications*, 18, 1, pp. 64-79.

Clark, R. N. and T. L. Roush (1984): "Reflectance spectroscopy: Quantitative analysis techniques for remote sensing applications," *Journal of Geophysical Research*, 89, pp. 6329-6340.

Curran, P. J., J. L. Dungan, *et al*. (2001): "Estimating the foliar biochemical concentration of leaves with reflectance spectrometry-testing the Kolaly and Clark methodologies", *Remote Sensing of Environment*, 76, pp. 349-359.

De Santis, A. and E. Chuvieco (2008): "Comparative analysis of different Satellite-Borne sensors to map burn severity in the Riba de Saelices (Guadalajara) fire", *Revista de Teledeteccion*, 29, pp. 25-37.

Debba, P., F. J. A. van Ruitenbeek, *et al*. (2005): "Optimal field sampling for targeting minerals using hyperspectral data", *Remote Sensing of Environment*, 99, pp. 373-386.

Eva, H. and E. F. Lambin (1998a): "Burned area mapping in Central Africa using ATSR data", *International Journal of Remote Sensing*, 19, pp. 3473-3497.

Fawcett, T. (2006): "An introduction to ROC analysis", *Pattern Recognition Letters*, 27, pp. 861-874.

Garcia, M. and E. Chuvieco (2004): "Assessment of the potential of SAC-C/MMRS imagery for mapping burned areas in Spain", *Remote Sensing of Environment*, 92, pp. 414–423.

Giglio, L., J. Descloitres, *et al*. (2003): "An Enhanced Contextual Fire Detection Algorithm for MODIS", *Remote Sensing of Environment*, 87, 2-3, pp. 273-282.

Giglio, L., T. Loboda, *et al*. (2009): "An active-fire based burned area mapping algorithm for the MODIS sensor", *Remote Sensing of Environment*, 113, pp. 408-420.

Oliva Pavón, P. y Chuvieco, E. (2013): "Assessment of the discrimination ability of MERIS spectral data for burned area mapping using ROC curves", GeoFocus (Artículos), nº 13-2, p. 41-65. ISSN: 1578-5157

Gonzalez-Alonso, F., S. Merino de Miguel, *et al*. (2007): "MERIS full resolution data for mapping level-of-damage caused by forest fires: the Valencia de Alcántara event in August 2003", *International Journal of Remote Sensing*, 28, 3-4, pp. 797-809.

González-Alonso, F., V. Salgado, *et al*. (2009): "Forest burn in China by means of MERIS and MODIS images", *Dragon 2 Symposium*, Barcelona (Spain).

Guanter, L., L. Gómez-Chova, *et al*. (2008): "Coupled retrieval of aerosol optical thickness, columnar water vapor and surface reflectance maps from ENVISAT/MERIS data over land", *Remote Sensing of Environment*, 112, pp. 2898-2913.

Holden, Z. A., A. M. S. Smith, *et al*. (2005): "Evaluation of novel thermally enhanced spectral indices for mapping fire perimeters and comparisons with fire atlas data", *International Journal of Remote Sensing*, 26, 21, pp. 4801-4808.

Huang, Z., B. J. Turner, *et al*. (2004): "Estimating foliage nitrogen concentration from HYMAP data using continuum removal analysis", *Remote Sensing of Environment*, 93, pp. 18-29.

Kailath, T. (1967): "The divergence and Bhattacharyya distance measures in signal selection", *IEEE Transactions on Communication Technology*, 15, 1, pp. 52-60.

Kaufman, Y. J. and L. A. Remer (1994): "Detection of forests using Mid-IR reflectance: an application for aerosol studies", *IEEE Transactions on Geoscience and Remote Sensing*, 32, 3, pp. 672-683.

Khanna, S., A. Palacios-Orueta, *et al*. (2007): "Development of angle indexes for soil moisture estimation, dry matter detection and land-cover discrimination", *Remote Sensing of Environment*, 109, pp. 154-165.

Koutsias, N. and M. Karteris (1998): "Logistic regression modelling of multitemporal Thematic Mapper data for burned area mapping", *International Journal of Remote Sensing*, 19, 18, pp. 3499-3514.

Koutsias, N. and M. Karteris (2000): "Burned area mapping using logistic regression modeling of a single post-fire Landsat-5 Thematic Mapper image", *International Journal of Remote Sensing*, 21, 4, pp. 673-687.

Kucera, J. and Y. Yoshifumi (2001): "Regional monitoring of forest disturbances and their potential effects to carbon cycling", *22nd Asian Conference on Remote Sensing*, Singapure, Centre for Remote Imaging, Sensing and Processing (CRISP), Asian Association on Remote Sensing (AARS).

Kumar, R. and L. F. Silva (1977): "Separability of agricultural cover types by remote sensing in the visible and infrared wavelength regions", *IEEE Transactions on Geoscience Electronics*, 15, 1, pp. 8.

López García, M. J. and V. Caselles (1991): "Mapping burns and natural reforestation using Thematic Mapper data", *Geocarto International*, 1, pp. 31-37.

Maggi, M. and D. Stroppiana (2002): "Advantages and drawbacks of NOAA-AVHRR and SPOT-VGT for burnt area mapping in a tropical savanna ecosystem", *Canadian Journal of Remote Sensing*, 28, 2, pp. 231-245.

Oliva Pavón, P. y Chuvieco, E. (2013): "Assessment of the discrimination ability of MERIS spectral data for burned area mapping using ROC curves", GeoFocus (Artículos), nº 13-2, p. 41-65. ISSN: 1578-5157

Martín, M. P. (1998): "Cartografía e inventario de incendios forestales en la península Ibérica a partir de imágenes NOAA-AVHRR", Univ. of Alcalá.

Mutanga, O., A. K. Skidmore, *et al*. (2004): "Predicting in situ pasture quality in the Kruger National Park, South Africa, using continuum-removed absorption features", *Remote Sensing of Environment*, 89, pp. 393-408.

Oliva, P., M. P. Martín, *et al*. (2011): "Burned area mapping with MERIS post-fire image", *International Journal of Remote Sensing*, 32, 15, pp. 26.

Oliva, P. and P. Martin (2007): "Mapping burned area by using Spectral Angle Mapper in MERIS images", *6th International workshop on remote Sensing and GIS Applications to Forest Fire Management: Fire Effects Assessment*, Thessaloniki, Greece, Aristotele University of Thessaloniki.

Pereira, J. M. C. (1999): "A comparative evaluation of NOAA/AVHRR vegetation indexes for burned surface detection and mapping", *IEEE Transactions on Geoscience and Remote Sensing*, 37, 1, pp. 217-226.

Pinty, B. and M. M. Verstraete (1992): "GEMI:a non-linear index to monitor global vegetation from satellites", *Vegetatio*, 101, pp. 15-20.

Pyne, S. J., P. L. Andrews, *et al*. (1996): *Introdution to Wildland fire*.Jonh Wiley & Sons, Inc.

Richards, J. A. (1984): "Thematic mapping from multitemporal image data using the Principal Components Transformation", *Remote Sensing of Environment*, 16, pp. 35-46.

Roldán-Zamarrón, A., S. Merino de Miguel, *et al*. (2006): "Minas de Rio Tinto (south Spain) forest fire: Burned area assessment and fire severity mapping using Landsat 5-TM, Envisat-MERIS, and Terra-MODIS postfire images", *Journal of Geophysical Research*, 111, G04S11.

Roy, D. P., Y. Jin, *et al*. (2005): "Prototyping a global algorithm for systematic fire-affected area mapping using MODIS time series data", *Remote Sensing of Environment*, 97, pp. 137-162.

Roy, D. P. and T. Landmann (2005): "Characterizing the surface heterogeneity of fire effects using multi-temporal reflective wavelength data", *International Journal of Remote Sensing*, 26, 19, pp. 4197-4218.

Silva, J. M. N., J. F. C. L. Cadima, *et al*. (2004): "Assessing the feasibility of a global model for multi-temporal burned area mapping using SPOT-VEGETATION", *International Journal of Remote Sensing*, 25, 22, pp. 4889-4913.

Smith, A. M. S., N. A. Drake, *et al*. (2007): "Production of Landsat ETM+ reference imagery of burned areas within Southern African savannahs: comparison of methods and application to MODIS", *International Journal of Remote Sensing*, 28, 12, pp. 2753-2775.

Stroppiana, D., S. Pinnick, *et al*. (2002): "Radiometric analysis of SPOT-VEGETATION images for burnt area detection in Northern Australia", *Remote Sensing of Environment*, 82, pp. 21-37.

Swets, J. A., R. M. Dawes, *et al*. (2000): "Better decisions through science", *Scientific American*, 283, pp. 82-87.

Tansey, K., J. M. Grégoire, *et al*. (2008): "A new, global, multi-annual (2000-2007) burnt area product at 1 km resolution", *Geophysical Research Letters*, 35, L01401, pp. 6.

Oliva Pavón, P. y Chuvieco, E. (2013): "Assessment of the discrimination ability of MERIS spectral data for burned area mapping using ROC curves", GeoFocus (Artículos), nº 13-2, p. 41-65. ISSN: 1578-5157

Trigg, S. and S. Flasse (2000): "Characterizing the spectral-temporal response of burned savannah using in situ spectroradiometry and infrared thermometry", *International Journal of Remote Sensing*, 21, 16, pp. 3161-3168.

Trigg, S. and S. Flasse (2001): "An evaluation of different bi-spectral spaces for discriminating burned shrub-savannah", *International Journal of Remote Sensing*, 22, 13, pp. 2641–2647.

van der Meer, F. D. (2000): "Spectral curve shape matching with a continuum removed CCSM algorithm", *International Journal of Remote Sensing*, 21, 16, pp. 3179-3185.

van der Werf, G. R., J. T. Randerson, *et al*. (2010): "Global fire emissions and the contribution of deforestation, savanna, forest, agricultural, and peat fires (1997-2009)", *Atmospheric Chemistry and Physics*, 10, pp. 11707-11735.

Veraverbeke, S., S. Harris, *et al*. (2011): "Evaluating spectral indices for burned area discrimination using MODIS/ASTER (MASTER) airborne simulator data", *Remote Sensing of Environment*, 115, 10, pp. 2702-2709.

Viedma, O., J. M. Moreno, *et al*. (2006): "Interactions between land use/land cover change, forest fires and landscape structure in Sierra de Gredos (Central Spain)", *Environmental Conservation*, 33, 3, pp. 212-222.

Zarco-Tejada, P. J., J. D. Miller, *et al*. (2004): "Needle chlorophyll content estimation through model inversion using hyperspectral data from boreal conifer forest canopies", *Remote Sensing of Environment*, 89, pp. 189-199.

Zarco-Tejada, P. J. and J. R. Miller (1999): "Land cover mapping at BOREAS using red edge spectral parameters from CASI imagery", *Journal of Geophysical Research*, 104, 22, pp. 27.921-927.933.